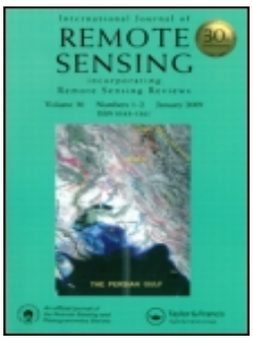

International Journal of Remote Sensing

ISSN: 0143-1161 (Print) 1366-5901 (Online) Journal homepage: http://www.tandfonline.com/loi/tres20

# Forest recovery trends derived from Landsat time series for North American boreal forests

Paul D. Pickell, Txomin Hermosilla, Ryan J. Frazier, Nicholas C. Coops & Michael A. Wulder

**To cite this article:** Paul D. Pickell, Txomin Hermosilla, Ryan J. Frazier, Nicholas C. Coops & Michael A. Wulder (2016) Forest recovery trends derived from Landsat time series for North American boreal forests, International Journal of Remote Sensing, 37:1, 138-149

**To link to this article:** http://dx.doi.org/10.1080/2150704X.2015.1126375

INTERNATIONAL JOURNAL OF REMOTE SENSING, 2015
VOL. 37, NO. 1, 138–149
http://dx.doi.org/10.1080/2150704X.2015.1126375

Taylor & Francis
Taylor & Francis Group



# Forest recovery trends derived from Landsat time series for North American boreal forests

Paul D. Pickell[a], Txomin Hermosilla[a], Ryan J. Frazier[a], Nicholas C. Coops[a] and Michael A. Wulder[b]

[a]Integrated Remote Sensing Studio, Department of Forest Resources Management, University of British Columbia, Vancouver, British Columbia, Canada; [b]Canadian Forest Service (Pacific Forestry Centre), Natural Resources Canada, Victoria, British Columbia, Canada



**ABSTRACT**

A critical component of landscape dynamics is the recovery of vegetation following disturbance. The objective of this research was to characterize the forest recovery trends associated with a range of spectral indicators and report their observed performance and identified limitations. Forest disturbances were mapped for a random sample of three major bioclimate zones of North American boreal forests. The mean number of years for forest to recover, defined as time required to for a pixel to attain 80% of the mean spectral value of the 2 years prior to disturbance, was estimated for each disturbed pixel. The majority of disturbed pixels recovered within the first 5 years regardless of the index ranging from approximately 78% with normalized burn ratio (NBR) to 95% with tasselled cap greenness (TCG) and after 10 years more than 93% of disturbed pixels had recovered. Recovery rates suggest that normalized differenced vegetation index (NDVI) and TCG saturate earlier than indices that emphasize longer wavelengths. Thus, indices such as NBR and the mid-infrared spectral band offer increased capacity to characterize different levels of forest recovery. The mean length of time for spectral indices to recover to 80% of the pre-disturbance value for pixels disturbed 10 or more years ago was highest for NBR, 5.6 years, and lowest for TCG, 1.7 years. The mid-infrared spectral band had the greatest difference in recovered pixels among bioclimate zones 1 year after disturbance, ranging from approximately 42% of disturbed pixels for the cold and mesic bioclimate zone to 60% for the extremely cold and mesic bioclimate zone. The cold and mesic bioclimate zone had the longest mean years to recover ranging from 1.9 years for TCG to 4.2 years for NBR, while the cool temperate and dry bioclimate zone had the shortest mean years to recover ranging from 1.6 years for TCG to 2.9 years for NBR suggesting differences in pre-disturbance conditions or successional processes. The results highlight the need for caution when selecting and interpreting a spectral index for recovery characterization, as spectral indices, based upon the constituent wavelengths, are sensitive to different vegetation conditions and will provide a variable representation of structural conditions of forests.

**ARTICLE HISTORY**
Received 4 June 2015
Accepted 18 November 2015

**CONTACT** Paul D. Pickell paul.pickell@forestry.ubc.ca Integrated Remote Sensing Studio, Department of Forest Resources Management, University of British Columbia, 2424 Main Mall, Vancouver, British Columbia V6T 1Z4, Canada

## 1. Introduction

The return of vegetation and initiation of successional processes, often called recovery, is a critical component of landscape dynamics (Frolking et al. 2009; Kennedy et al. 2012). Vegetation recovery is a process, not a state; as such, tools and measures that allow for capturing and relating this regeneration and related increase in structural complexity are required (Shatford, Hibbs, and Puettmann 2007). Time series remote sensing is ideally suited for systematic and transparent capture and description of recovery processes for forested ecosystems. From a remote sensing perspective, vegetation recovery has been defined for specific applications or objectives (Buma 2012; Frolking et al. 2009; Oliver and Larson 1996). For example, previous studies have defined recovery as: a factor of time since last disturbance (Kennedy et al. 2012); spectrally using time series trends (Hermosilla et al. 2015a; Schroeder et al. 2011; Kennedy, Yang, and Cohen 2010); and the required time to meet certain forest management-based conditions such as potential height, canopy cover, or stocking (LePage and Banner 2014; Franklin et al. 2002). Additionally, the structural attributes of vegetation recovery can be characterized using synthetic aperture radar (Saatchi and Moghaddam 2000), light detection and ranging (Bolton, Coops, and Wulder 2015), and passive stereo optical remote sensing (Persson et al. 2013). Although all these definitions are valid, the objectives of any study considering time series spectrally based recovery trajectories must be carefully considered, articulated, and linked in a meaningful way to the spectral values or indices used. Additionally, it is critical that the limitations associated with each definition and related methods applied are sufficiently described.

Subtle differences among spectrally based recovery indicators can affect the conclusions of a study. Many remote sensing based definitions of recovery have used the normalized differenced vegetation index (NDVI) (Tucker 1979; Cuevas-Gonzalez et al. 2009; Sader et al. 1989). Although NDVI is particularly sensitive to changes in foliar condition and is commonly used in disturbance detection applications (Nemani and Running 1997), it has demonstrated limitations as an indicator of recovery (Sader et al. 1989; Huete et al. 1997) largely because forbs, grasses, and other non-woody pioneer vegetation will immediately colonize a disturbed site and rapidly return the site to pre-disturbance NDVI levels (Buma 2012; Schroeder et al. 2011). Thus, NDVI provides limited capacity for characterization of structural attributes, which are often more important indicators for biodiversity, habitat availability, and carbon (Pflugmacher et al. 2014; Banskota et al. 2014). An improved understanding of the information content of particular vegetation indices suggests the use of indices that include short-wave infrared wavelengths (Cohen and Goward 2004; Schroeder et al. 2011).

The objective of this research was to examine trends associated with a range of spectral indicators of forest recovery and report the potential limitations and caveats associated with each indicator. We present the results of a comparative analysis of spectrally derived indicators of forest recovery captured with a high level of spatial detail and utilizing a quarter century of Landsat imagery for a range of conditions across North American boreal forests.

## 2. Data and methods

This research utilizes the free and open access to imagery available from the United States Geological Survey (https://espa.cr.usgs.gov) and the Landsat satellite programme (Woodcock et al. 2008; Wulder et al. 2012). Landsat surface reflectance images derived from the Landsat

Ecosystem Disturbance Adaptive Processing System (Masek et al. 2008) with less than 70% cloud cover during the growing season were downloaded for a random sample of 40 World Reference System 2 (WRS-2) scenes (Figure 1) for the period 1985–2010. The sample was randomly stratified by three major bioclimate zones and intersected with the North American boreal zone (Metzger et al. 2013, Brandt 2009). We calculated the length of the growing season for each scene based on the scene centre latitude (Zhou et al. 2001). Peak NDVI day-of-year was derived from moderate resolution spectroradiometer (MODIS) imagery for North America and was equivalent to the target day-of-year for the best available pixel (BAP) compositing: July 28 (Zeng, Jia, and Epstein 2011). By coupling length of the growing season with peak NDVI day-of-year, we derived the start- and end-of-season days-of-year. Thus, the growing season was dynamically defined for each scene in order to accommodate latitudinal shift in growing season timing and length and to ensure that the Landsat imagery was phenologically consistent across the time series.

We used a BAP approach to create image composites to reduce data gaps in the image time series caused by cloud, cloud shadow, haze, and smoke (White et al. 2014). The image compositing method scores pixels from the multiple Landsat image acquisitions based on sensor, day-of-year, atmospheric opacity, and proximity to cloud or cloud shadow using the criteria given in White et al. (2014). Pixels identified by the Fmask algorithm (Zhu and Woodcock 2012) as cloud, shadow, or snow were masked from the BAP composites and a 50 m buffer was applied around clouds and cloud shadows to reduce misclassification errors. The Landsat Thematic Mapper (TM) sensor was scored higher than the Enhanced Thematic Mapper Plus (ETM+) sensor due to the scan line corrector malfunction that occurred with the ETM+ in May of 2003. Day-of-year was scored according to a Gaussian function with a maximum score equivalent to the

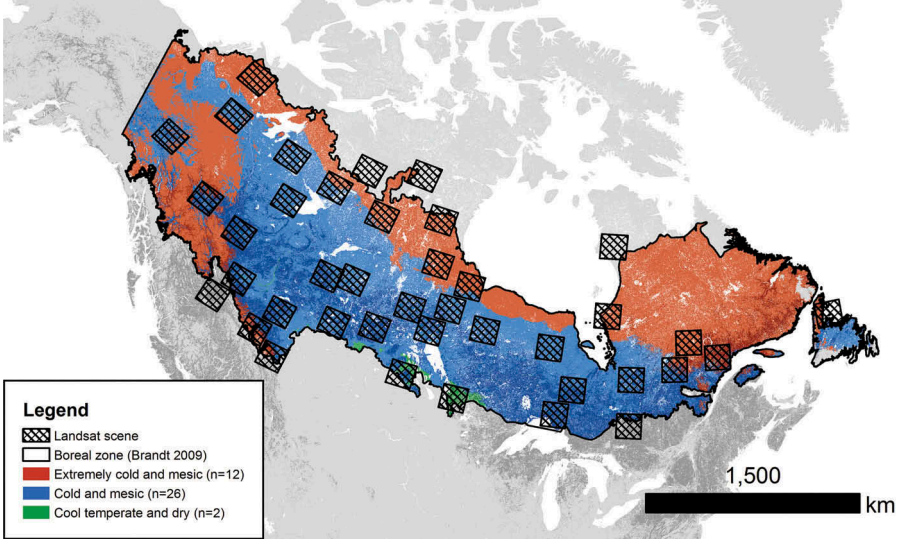


**Figure 1.** Distribution of the Landsat scenes stratified across major bioclimate zones (Metzger et al. 2013) within North American boreal forests (Brandt 2009). The bioclimate zones are transparent relative to the 2000 MODIS vegetation continuous fields (VCF) layer depicting pixels greater than 50% forested (dark grey).

median day-of-year of the growing season. Pixels with atmospheric opacity lower than 10% were scored higher to avoid the selection of hazy observations. The pixels with the highest scores based on these criteria were then composited into annual images that were used in the disturbance and recovery mapping process (White et al. 2014).

Forest disturbances were mapped using a modified version of the vegetation change tracker (VCT, after Huang et al. 2010) for the time series of each target WRS-2 path row (Pickell et al. 2014). The modified VCT assigns a class of *persisting forest, persisting non-forest, disturbed*, or *water* for each pixel in the time series using trend logic applied to a spectral index. First, a forest training mask is created for each annual image composite and then a spectral index is computed for the time series of forested pixels. Thresholds are set *a priori* to determine whether a forested pixel will be assigned to the disturbed or stable forest classes. Forest training areas were identified using a combination of MODIS Vegetation Continuous Fields (MOD44B) product from the year 2000 (Sexton et al. 2013), annual NDVI values, and visual interpretation of true-colour annual Landsat composites. Although the VCT analysis relied in part on annual NDVI values to map initial forest training areas, NDVI was not used to map disturbances and thus this choice was not related to the evaluation of NDVI as a recovery indicator. The disturbance index (DI) (Healey et al. 2005) was used for mapping forest disturbances and identifying core forested areas with thresholds that were developed specifically for boreal forests (Pickell et al. 2014). Pixels that exceeded the DI thresholds for at least 3 consecutive years were labelled as *disturbed*. We only considered stand-replacing disturbance from fire and forest harvesting because forest structure changes significantly following greater magnitude disturbance severities (Hermosilla et al. 2015b) and vegetation recovery can therefore be robustly characterized (Schroeder et al. 2011). Moreover, the VCT captures a range of forest disturbances with varying severities at lower accuracies (Thomas et al. 2011). Disturbed pixels with a DI magnitude change of at least 5 were included in the final analysis as stand-replacing disturbances (Healey et al. 2005). Pixels disturbed in multiple years were not considered and only the most recent disturbances of the time series were included in the final analysis. Disturbance was filtered to a minimum mapping unit of 12 Landsat pixels (~1 ha). Previous studies have demonstrated the spatial accuracy of the VCT-derived disturbance maps to be very high for stand-replacing disturbance (>90% accuracy by area) and the times of occurrence of the majority of disturbance events were correctly identified within ±1 year (Pickell et al. 2014; Thomas et al. 2011).

A suite of spectral indices were selected to represent a range of spectral responses of vegetation recovery: NDVI; normalized burn ratio (NBR) (Key and Benson 2006); tasselled cap greenness (TCG) (Crist 1985); and the mid-infrared Landsat band 5 (B5) (Schroeder et al. 2011). Recovery was defined as 80% of the mean spectral value of the 2 years prior to disturbance for each disturbed pixel in the time series. This definition is similar to other spectrally based forest recovery definitions (e.g. Kennedy et al. 2012; Baumann et al. 2012; Schroeder et al. 2011). Two years of pre-disturbance observations represented a compromise between characterizing recovery trends for as much of the time series as possible while using stable pre-disturbance trends that were reliable and representative of characteristics present at the pixel level. Thus, recovery was not quantified for disturbances occurring in the last year of the time series.

## 3. Results and discussion

Trends in recovery varied depending on the indicator and bioclimate zone. TCG and NDVI provided the fastest recovery rates, while NBR and the mid-infrared spectral band provided the slowest recovery rates. The mean length of time for spectral indices to recover (reach 80% of their pre-disturbance value) was highest for NBR, 3.9 years, and lowest for TCG, 1.7 years. The cold and mesic bioclimate zone had the longest mean years to recover ranging from 1.9 years for TCG to 4.2 years for NBR, while the cool temperate and dry bioclimate zone had the shortest mean years to recover ranging from 1.6 years for TCG to 2.9 years for NBR. This result may indicate that return of vegetation and initiation of successional processes is at least partially dependent on bioclimate zone, but the indices are also correlated. For example, the mid-infrared spectral band is a major component in the calculation of NBR, and NDVI describes the contrast between the reflectances in the visible red and near-infrared spectral bands which also receive the largest weightings in the calculation of TCG. It is important to note that the number of pixels recovered is a function of number of years since disturbance. For example, only disturbances that occurred between 1987 and 1998 could have had recovery trends beyond a 10-year horizon. Therefore, the number of pixels recovered is necessarily biased towards shorter recovery times in the time series. Mean years to recover was higher for the subset of pixels that were disturbed 10 or more years ago (i.e. between 1987 and 1998): 5.6 years for NBR; 4.8 years for the mid-infrared spectral band; 2.7 years for NDVI; and 1.7 years for TCG.

The majority of pixels detected as disturbed had observable trends of vegetation recovery within the first 5 years of disturbance regardless of the index or bioclimate zone. Figure 2 shows the frequency of recovered pixels relative to the years since disturbance by bioclimate zone. There was little difference between bioclimate zones for the same index with most differences observed within the first 5 years of disturbance (Figure 2). The mid-infrared spectral band had the greatest difference among bioclimate zones 1 year after disturbance, ranging from 42.2% for the cold and mesic bioclimate zone to 59.9% for the extremely cold and mesic bioclimate zone (Figure 2). The cumulative percentage of pixels recovered after 5 years was greater for NDVI (93.4%) and TCG (95.3%) compared with NBR (77.9%) and the mid-infrared spectral band (84.3%). The differences of cumulative percentage of pixels recovered were minimal after 10 years between NBR (93.2%), the mid-infrared spectral band (93.1%), NDVI (99.5%), and TCG (98.5%). These results indicate that vegetation has spectrally returned to pre-disturbance levels and that successional processes are likely to have initiated. Sites taking more time to recover may have experienced a land use change or a notably severe disturbance.

The percentage of pixels that had not recovered after 5 years were plotted as a function of the percentage of the pre-disturbance mean value for each index in Figure 3 where 80% corresponded to 80% of the mean pre-disturbance values of the recovery indicator. After 5 years, the majority of disturbed pixels in the extremely cold and mesic and the cold and mesic bioclimate zones for NDVI and the mid-infrared spectral band were close to meeting the 80% threshold (Figure 3). The trend in recovering pixels for TCG was similar to NBR (Figure 3), but the relative difference in cumulative recovered pixels after 5 years between these indices was 17.4%. Disturbed pixels in the extremely cold and mesic and cold and mesic bioclimate zones had higher rates of recovery compared with the cool temperate and dry bioclimate zone (Figure 3).

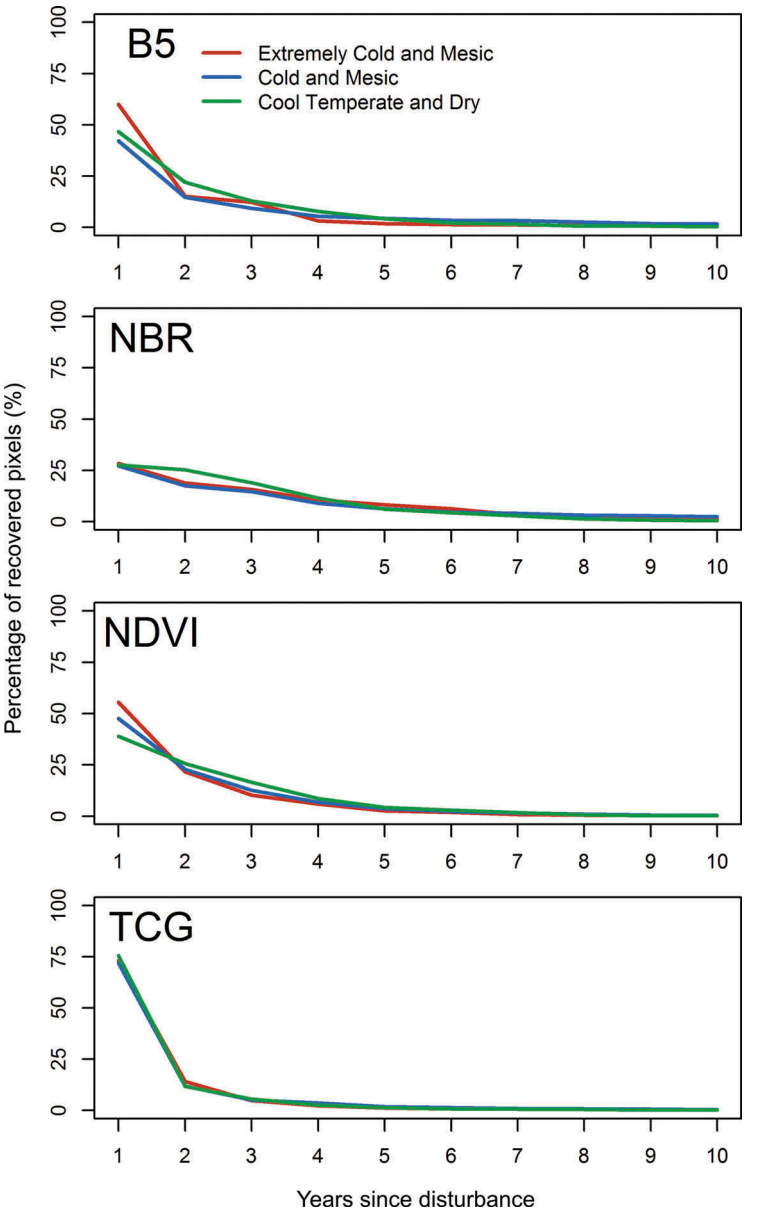


**Figure 2.** Percentage of pixels recovered by the number of years following disturbance. The number of disturbed pixels is equal for all indices.

The mid-infrared spectral band and NBR have been shown to be related to structural components of vegetation, while NDVI and TCG are more sensitive to levels of chlorophyll (Cuevas-Gonzalez et al. 2009; Epting and Verbyla 2005). Both the mid-infrared spectral band and NBR are known to represent the recovery of non-leafy structural attributes of vegetation beyond the initial flush of grasses, herbs, and shrubs (Wulder 1998; Schroeder et al. 2011). The curves of non-recovered pixels for the mid-infrared band and NDVI likely represent variation of spectral recovery across a gradient of disturbance severity (Figure 3). By contrast,

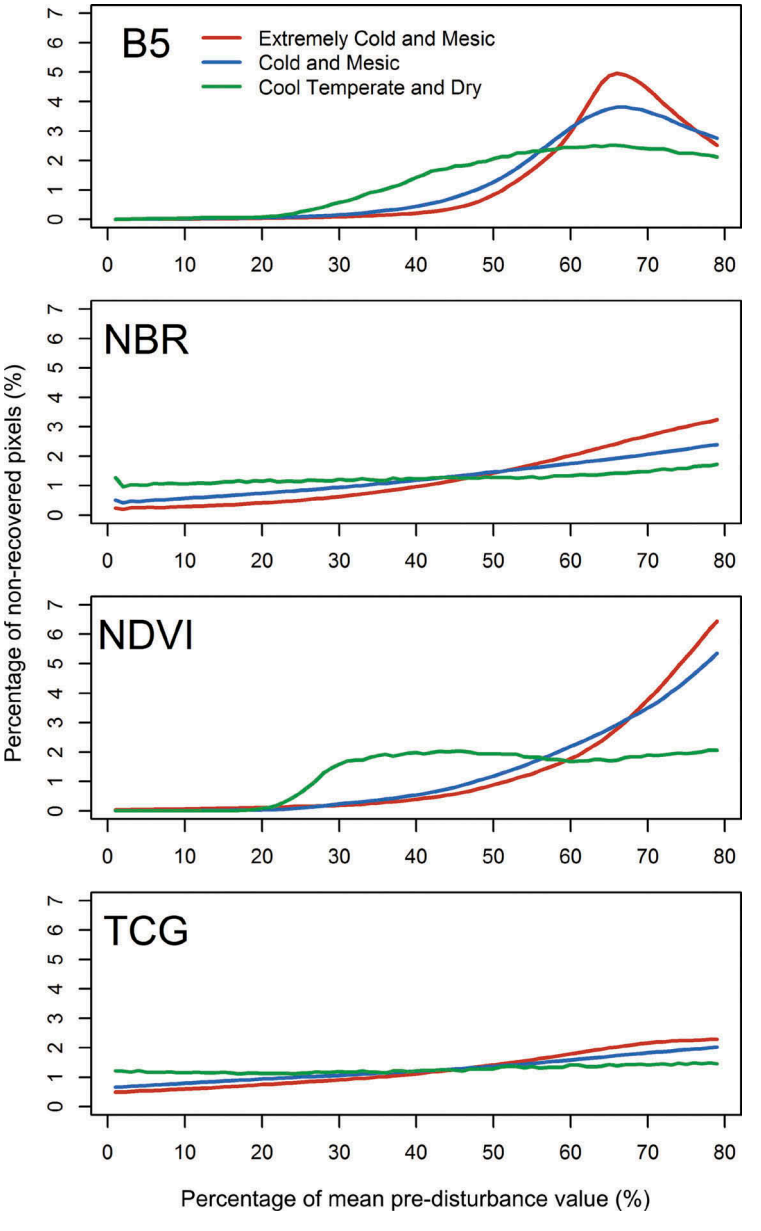


**Figure 3.** Percentage of non-recovered pixels against percentage of the mean pre-disturbance value for each index investigated 5 years after disturbance.

the linear curves of NBR and TCG are likely an artefact of continually increasing near-infrared reflectance as leaf cover accumulates within the disturbed pixel (Figure 3). Thus, the results indicate that the mid-infrared spectral band and NBR are expected to be more suitable for tracking vegetation succession following disturbance when compared to NDVI and TCG. Based on knowledge of successional processes (Oliver 1980), the signal from visible and near-infrared wavelengths is expected to quickly saturate following disturbance due to the rapid colonization of early pioneer and shade-intolerant species.

Recovery rates among the bioclimate zones suggest that there may be subtle spectral differences in successional processes. For example, Figure 2 shows the frequency of recovered pixels for NDVI and the mid-infrared spectral band provided improved opportunities to observe differences between the bioclimate zones in the first 5 years post-disturbance. The higher rate of recovery observed for the extremely cold and mesic bioclimate zone in the first year post-disturbance could be related with lower pre-disturbance mean values compared to the other zones when using the mid-infrared spectral band and NDVI. Also, the accuracy of the VCT has not been tested in sparse boreal forests and the forest-tundra ecotone that characterizes much of the extremely cold and mesic bioclimate zone and more research is needed in this area. Trends in NBR recovery were much more gradual while TCG saturated 1 year after disturbance (Figure 2).

Recovery rates among the bioclimate zones during later succession (i.e. ≥5 years post-disturbance) were also best observed using NDVI and the mid-infrared spectral band (Figure 3). There was a notable lag effect for recovery of disturbed pixels in the cool temperate and dry bioclimate zone after 5 years with the mid-infrared spectral band and NDVI indices compared with the other bioclimate zones (Figure 3). The frequency distribution of non-recovered pixels in the cool temperate and dry bioclimate zone suggests that after 5 years these forests may still be far from reaching the recovery definition with the mid-infrared spectral band and NDVI (Figure 3).

The results should be interpreted with some caution because recovery was not distinguished for different disturbance types. It was evident that the choice of recovery indicator was important for different types of disturbance. For example, the initial flush of leafy vegetation following a fire or harvest saturates the recovery signal for NDVI and TCG. Additionally, disturbance legacies are evident in the recovery rates from visual assessment of harvesting and fire (Figure 4). For example, roads within harvests appear to recover more slowly than the surrounding forest using NDVI compared with TCG (Figure 4(a)). Recovery is remarkably heterogeneous within fires, which is primarily evident with the mid-infrared spectral band and NBR indices (Figure 4(b)). The examples shown in Figure 4

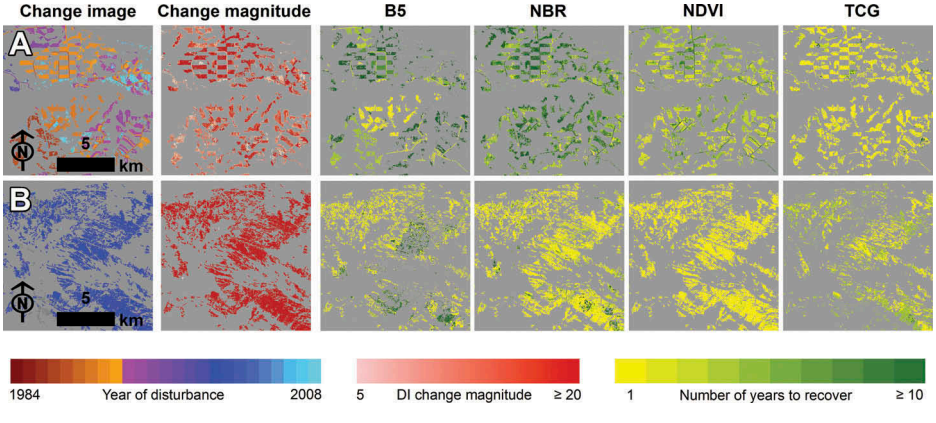


**Figure 4.** Number of years to recover by index for examples of forest harvesting in Alberta (a, path45/row23, 117° 17′ W 53° 44′ N) and a fire in Northwest Territories, Canada (b, path57/row14, 128° 12′ W 65° 33′ N). The year of disturbance colour ramp applies to the change image, the DI change magnitude colour ramp applies to the change magnitude image, and the number of years to recover colour ramp applies to the recovery images.

are typical of forest management occurring in southern boreal forests and fire which is much more common in occurrence and extent throughout the northern boreal forests.

## 4. Conclusions

In this paper, we analysed the implications of considering four spectral indices (NDVI, NBR, TCG, and the mid-infrared spectral band) to estimate forest recovery rates for boreal forests of North America using Landsat time series. The results indicated that spectral indices characterized different components of forest recovery. Thus, NDVI and TCG were related with the initial flush of leafy vegetation, while NBR and the mid-infrared spectral band were related with structural components caused by increasing structural complexity of the forest cover. Recovery time varied by indicator with NBR having the highest mean years to recover (3.9 years) and TCG having the lowest mean years to recover (1.7 years) across all bioclimate zones. The cold and mesic bioclimate zone had the slowest recovery rates across the indicators (ranging from 1.8 years for TCG to 4.1 years for NBR), while the cool temperate and dry bioclimate zone had the quickest recovery rates (ranging from 1.6 years for TCG to 2.9 years for NBR). Recovery time was remarkably heterogeneous within different disturbance types and was dependent on the indicator. Roads within harvests recovered more slowly than the surrounding forest and this was mostly evident with the mid-infrared spectral band and NBR. Fires were particularly heterogeneous using NDVI as a recovery indicator, but NBR and the mid-infrared spectral band showed improvement in distinguishing areas that took the longest to recover. We note that imagery is often not used in isolation and supplementing optical observations with active remote sensing measurements that can provide structure information could enhance estimation of regrowth with disturbance history from Landsat. Regardless, the results presented here can advance the assessment and monitoring of forest recovery for large area mapping initiatives and improve our understanding of post-disturbance vegetation dynamics in North American boreal forests.

## Acknowledgements

We thank the US Geological Survey for providing open access to the Landsat archive and the Earth Resources Observation and Science data centre for processing the Landsat surface reflectance products. Jeffrey Masek and Shannon Franks provided the Vegetation Change Tracker programme that was modified from Chengquang Huang's original algorithm.

## Disclosure statement

No potential conflict of interest was reported by the authors.

## References

Banskota, A., N. Kayastha, M. J. Falkowski, M. A. Wulder, R. E. Froese, and J. C. White. 2014. "Forest Monitoring Using Landsat Time Series Data: A Review." *Canadian Journal of Remote Sensing* 40: 362–384. doi:10.1080/07038992.2014.987376.

Baumann, M., M. Ozdogan, T. Kuemmerle, K. J. Wendland, E. Esipova, and V. C. Radeloff. 2012. "Using the Landsat Record to Detect Forest-Cover Changes during and after the Collapse of the Soviet Union in the Temperate Zone of European Russia." *Remote Sensing of Environment* 124: 174–184. doi:10.1016/j.rse.2012.05.001.

Bolton, D. K., N. C. Coops, and M. A. Wulder. 2015. "Characterizing Residual Structure and Forest Recovery following High-Severity Fire in the Western Boreal of Canada Using Landsat Time-Series and Airborne Lidar Data." *Remote Sensing of Environment* 163: 48–60. doi:10.1016/j.rse.2015.03.004.

Brandt, J. P. 2009. "The Extent of the North American Boreal Zone." *Environmental Reviews* 17: 101–161. doi:10.1139/A09-004.

Buma, B. 2012. "Evaluating the Utility and Seasonality of NDVI Values for Assessing Post-Disturbance Recovery in a Subalpine Forest." *Environmental Monitoring and Assessment* 184: 3849–3860. doi:10.1007/s10661-011-2228-y.

Cohen, W. B., and S. N. Goward. 2004. "Landsat's Role in Ecological Applications of Remote Sensing." *BioScience* 54: 535–545. doi:10.1641/0006-3568(2004)054[0535:LRIEAO]2.0.CO;2.

Crist, E. P. 1985. "A TM Tasseled Cap Equivalent Transformation for Reflectance Factor Data." *Remote Sensing of Environment* 17: 301–306. doi:10.1016/0034-4257(85)90102-6.

Cuevas-Gonzalez, M., F. Gerard, H. Balzter, and D. Riaño. 2009. "Analysing Forest Recovery after Wildfire Disturbance in Boreal Siberia Using Remotely Sensed Vegetation Indices." *Global Change Biology* 15: 561–577. doi:10.1111/j.1365-2486.2008.01784.x.

Epting, J., and D. L. Verbyla. 2005. "Landscape Level Interactions of Pre-Fire Vegetation, Burn Severity, and Post-Fire Vegetation over a 16-Year Period in Interior Alaska." *Canadian Journal of Forest Research* 35: 1367–1377. doi:10.1139/x05-060.

Franklin, J. F., T. A. Spies, R. Van Pelt, A. B. Carey, D. A. Thornburgh, D. R. Berg, D. B. Lindenmayer, et al. 2002. "Disturbances and Structural Development of Natural Forest Ecosystems with Silvicultural Implications, Using Douglas-Fir Forests as an Example." *Forest Ecology and Management* 155: 399–423. doi:10.1016/S0378-1127(01)00575-8.

Frolking, S., M. W. Palace, D. B. Clark, J. Q. Chambers, H. H. Shugart, and G. C. Hurtt. 2009. "Forest Disturbance and Recovery: A General Review in the Context of Spaceborne Remote Sensing of Impacts on Aboveground Biomass and Canopy Structure." *Journal of Geophysical Research: Biogeosciences* 114 (G00E02). doi:10.1029/2008JG000911.

Healey, S. P., W. B. Cohen, Y. Zhiqiang, and O. N. Krankina. 2005. "Comparison of Tasseled Cap-Based Landsat Data Structures for Use in Forest Disturbance Detection." *Remote Sensing of Environment* 97: 301–310. doi:10.1016/j.rse.2005.05.009.

Hermosilla, T., M. A. Wulder, J. C. White, N. C. Coops, and G. W. Hobart. 2015a. "An Integrated Landsat Time Series Protocol for Change Detection and Generation of Annual Gap-Free Surface Reflectance Composites." *Remote Sensing of Environment* 158: 220–234. doi:10.1016/j.rse.2014.11.005.

Hermosilla, T., M. A. Wulder, J. C. White, N. C. Coops, and G. W. Hobart. 2015b. "Regional Detection, Characterization, and Attribution of Annual Forest Change from 1984 to 2012 Using Landsat-Derived Time-Series Metrics." *Remote Sensing of Environment* 170: 121–132. doi:10.1016/j.rse.2015.09.004.

Huang, C., S. N. Goward, J. G. Masek, N. Thomas, Z. Zhu, and J. E. Vogelmann. 2010. "An Automated Approach for Reconstructing Recent Forest Disturbance History Using Dense Landsat Time Series Stacks." *Remote Sensing of Environment* 114: 183–198. doi:10.1016/j.rse.2009.08.017.

Huete, A. R., H. Q. Liu, K. Batchily, and W. J. D. A. Van Leeuwen. 1997. "A Comparison of Vegetation Indices over a Global Set of TM Images for EOS-MODIS." *Remote Sensing of Environment* 59: 440–451. doi:10.1016/S0034-4257(96)00112-5.

Kennedy, R. E., Z. Yang, and W. B. Cohen. 2010. "Detecting Trends in Forest Disturbance and Recovery Using Yearly Landsat Time Series: 1. Landtrendr – Temporal Segmentation Algorithms." *Remote Sensing of Environment* 114: 2897–2910. doi:10.1016/j.rse.2010.07.008.

Kennedy, R. E., Z. Yang, W. B. Cohen, E. Pfaff, J. Braaten, and P. Nelson. 2012. "Spatial and Temporal Patterns of Forest Disturbance and Regrowth within the Area of the Northwest Forest Plan." *Remote Sensing of Environment* 122: 117–133. doi:10.1016/j.rse.2011.09.024.

Key, C. H., and N. C. Benson. 2006. *Landscape Assessment (LA): Sampling and Analysis Methods*. Fort Collins, CO: USDA Forest Service General Technical Report. RMRS-GTR-164-CD.

LePage, P., and A. Banner. 2014. "Long-Term Recovery of Forest Structure and Composition after Harvesting in the Coastal Temperate Rainforests of Northern British Columbia." *Forest Ecology and Management* 318: 250–260. doi:10.1016/j.foreco.2014.01.031.

Masek, J. G., S. N. Goward, R. E. Kennedy, W. B. Cohen, G. G. Moisen, K. Schleeweis, and C. Huang. 2013. "United States Forest Disturbance Trends Observed Using Landsat Time Series." *Ecosystems* 16: 1087–1104. doi:10.1007/s10021-013-9669-9.

Metzger, M. J., R. G. H. Bunce, R. H. G. Jongman, R. Sayre, A. Trabucco, R. Comer, and M. Sykes. 2013. "A High-Resolution Bioclimate Map of the World: A Unifying Framework for Global Biodiversity Research and Monitoring." *Global Ecology and Biogeography* 22 (5): 630–638. doi:10.1111/geb.12022.

Nemani, R., and S. Running. 1997. "Land Cover Characterization Using Multitemporal Red, Near-IR, and Thermal-IR Data from NOAA/AVHRR." *Ecological Applications* 7: 79–90. doi:10.1890/1051-0761(1997)007[0079:LCCUMR]2.0.CO;2.

Oliver, C. D. 1980. "Forest Development in North America following Major Disturbances." *Forest Ecology and Management* 3: 153–168. doi:10.1016/0378-1127(80)90013-4.

Oliver, C. D., and B. C. Larson. 1996. *Forest Stand Dynamics*. New York, NY: John Wiley and Sons.

Persson, H., J. Wallerman, H. Olsson, and J. E. S. Fransson. 2013. "Estimating Forest Biomass and Height Using Optical Stereo Satellite Data and a DTM from Laser Scanning Data." *Canadian Journal of Remote Sensing* 39: 251–262. doi:10.5589/m13-032.

Pflugmacher, D., W. B. Cohen, R. E. Kennedy, and Z. Yang. 2014. "Using Landsat-Derived Disturbance and Recovery History and Lidar to Map Forest Biomass Dynamics." *Remote Sensing of Environment* 151: 124–137. doi:10.1016/j.rse.2013.05.033.

Pickell, P. D., T. Hermosilla, N. C. Coops, J. G. Masek, S. Franks, and C. Huang. 2014. "Monitoring Anthropogenic Disturbance Trends in an Industrialized Boreal Forest with Landsat Time Series." *Remote Sensing Letters* 5 (9): 783–792. doi:10.1080/2150704X.2014.967881.

Saatchi, S. S., and M. Moghaddam. 2000. "Estimation of Crown and Stem Water Content and Biomass of Boreal Forest Using Polarimetric SAR Imagery." *IEEE Transactions on Geoscience and Remote Sensing* 38: 697–709. doi:10.1109/36.841999.

Sader, S. A., R. B. Waide, W. T. Lawrence, and A. T. Joyce. 1989. "Tropical Forest Biomass and Successional Age Class Relationships to a Vegetation Index Derived from Landsat TM Data." *Remote Sensing of Environment* 28: 143–198. doi:10.1016/0034-4257(89)90112-0.

Schroeder, T. A., M. A. Wulder, S. P. Healey, and G. G. Moisen. 2011. "Mapping Wildfire and Clearcut Harvest Disturbances in Boreal Forests with Landsat Time Series Data." *Remote Sensing of Environment* 115: 1421–1433. doi:10.1016/j.rse.2011.01.022.

Sexton, J. O., X.-P. Song, M. Feng, P. Noojipady, A. Anand, C. Huang, D.-H. Kim, et al. 2013. "Global, 30-M Resolution Continuous Fields of Tree Cover: Landsat-Based Rescaling of MODIS Vegetation Continuous Fields with Lidar-Based Estimates of Error." *International Journal of Digital Earth* 6: 427–448. doi:10.1080/17538947.2013.786146.

Shatford, J. P. A., D. E. Hibbs, and K. J. Puettmann. 2007. "Conifer Regeneration after Forest Fire in the Klamath-Siskiyous: How Much, How Soon?" *Journal of Forestry* 105: 139–146.

Thomas, N. E., C. Huang, S. N. Goward, S. Powell, K. Rishmawi, K. Schleeweis, and A. Hinds. 2011. "Validation of North American Forest Disturbance Dynamics Derived from Landsat Time Series Stacks." *Remote Sensing of Environment* 115: 19–32. doi:10.1016/j.rse.2010.07.009.

Tucker, C. J. 1979. "Red and Photographic Infrared Linear Combinations for Monitoring Vegetation." *Remote Sensing of Environment* 8: 127–150. doi:10.1016/0034-4257(79)90013-0.

White, J. C., M. A. Wulder, G. W. Hobart, J. E. Luther, T. Hermosilla, P. Griffiths, N. C. Coops, et al. 2014. "Pixel-Based Image Compositing for Large-Area Dense Time Series Applications and Science." *Canadian Journal of Remote Sensing* 40 (3): 192–212. doi:10.1080/07038992.2014.945827.

Woodcock, C. E., R. Allen, M. Anderson, A. Belward, R. Bindschadler, W. Cohen, F. Gao, et al. 2008. "Free Access to Landsat Imagery." *Science* 320 (5879): 1011. doi:10.1126/science.320.5879.1011a.

Wulder, M. A. 1998. "Optical Remote-Sensing Techniques for the Assessment of Forest Inventory and Biophysical Parameters." *Progress in Physical Geography* 22: 449–476. doi:10.1177/030913339802200402.

Wulder, M. A., J. G. Masek, W. B. Cohen, T. R. Loveland, and C. E. Woodcock. 2012. "Opening the Archive: How Free Data Has Enabled the Science and Monitoring Promise of Landsat." *Remote Sensing of Environment* 122: 2–10. doi:10.1016/j.rse.2012.01.010.

Zeng, H., G. Jia, and H. Epstein. 2011. "Recent Changes in Phenology over the Northern High Latitudes Detected from Multi-Satellite Data." *Environmental Research Letters* 6 (4): 045508. doi:10.1088/1748-9326/6/4/045508.

Zhou, L., C. J. Tucker, R. K. Kaufmann, D. Slayback, N. V. Shabanov, and R. B. Myneni. 2001. "Variations in Northern Vegetation Activity Inferred from Satellite Data of Vegetation Index during 1981 to 1999." *Journal of Geophysical Research* 106 (D17): 20069–20083. doi:10.1029/2000JD000115.

Zhu, Z., and C. E. Woodcock. 2012. "Object-Based Cloud and Cloud Shadow Detection in Landsat Imagery." *Remote Sensing of Environment* 118: 83–94. doi:10.1016/j.rse.2011.10.028.